

AUTOMATIC LIVER SEGMENTATION USING MEAN-SHIFT TECHNIQUES

SUDHA.P., Student,
Dr. T. Arumuga Maria Devi BE, M., Tech., Ph.D.,
AP-CITE,
Manonmaniam Sundaranar University,
Abishekapatti, Tirunelveli.

Abstract—In this paper, I present an auto context model (ACM)-based automatic liver segmentation algorithm, which combines ACM, multiatlases, and mean-shift techniques to segment liver from 3-D CT images. Our algorithm is a learning-based method and can be divided into two stages. At the first stage, i.e., the training stage, ACM is performed to learn a sequence of classifiers in each atlas space (based on each atlas and other aligned atlases). With the use of multiple atlases, multiple sequences of ACM-based classifiers are obtained. At the second stage, i.e., the segmentation stage, the test image will be segmented in each atlas space by applying each sequence of ACM-based classifiers. The final segmentation result will be obtained by fusing segmentation results from all atlas spaces via a multi classifier fusion technique. Specially, in order to speed up segmentation, given a test image, I first use an improved mean-shift algorithm to perform over segmentation and then implement the region-based image labeling instead of the original inefficient pixel-based image labeling. The proposed method is evaluated on the datasets of MICCAI 2007 liver segmentation challenge. The experimental results show that the average volume overlap error and the average surface distance achieved by our method are 8.3% and 1.5 mm, respectively, which are comparable to the results reported in the existing state-of-the-art work on liver segmentation.

Index Terms—Auto context model (ACM), fuzzy integral, liver segmentation, mean shift, multi classifier fusion, multiple atlases.

I. INTRODUCTION

ACCURATE segmentation of liver tissue from medical images is an essential and crucial step for computer-aided liver disease diagnosis and surgical planning. Among the various medical imaging techniques, computed tomography (CT) images are often used for these purposes, thanks to their high signal-to-noise ratio and better spatial resolution. However, liver segmentation from CT images is a challenging task, due to the high-intensity similarity between liver tissue and adjacent organs, the highly varying shape of the liver, and the presence of severe pathologies.

So far, numerous methods have been proposed for liver segmentation from CT images, such as those based on statistical shape models (SSMs) [1]–[5], those based on probabilistic atlases [6]–[8], those based on deformable models [9]–[20], those based on graph-cuts [21], those based on region growing [22], [23], threshold-based methods [24], [25], rule-

based methods [26], and learning-based methods [27]–[29]. Also, several good reviews can be found in [30] and [31].

Among all these liver segmentation methods, the SSM-based methods are currently the main automatic liver segmentation methods. Kainmuller et al. [2] employed SSM in combination

with a model of the typical intensity distribution around the liver boundary and neighboring structures. The SSM consisted of around 7000 landmarks and was built from an extensive training set of 112 liver shapes. The required correspondences were determined using a semiautomatic method, where the principal ridges of each liver were specified manually. Heimann et al. [3] incorporated SSM with an evolutionary algorithm to provide initialization for a deformable mesh that searches for human liver boundaries. The underlying SSM consisted of 2500 landmarks and was built automatically from 35 training shapes. Correspondences were determined by a population-based optimization approach. Zhang et al. [4] presented an approach for automatic liver segmentation from CT scans, which was based on a SSM integrated with an optimal surface detection strategy. In their work, a 3-D generalized Hough transform was employed to detect approximate location of the liver shape model. After the SSM initialization, the shape model was deformed to adapt to the liver contour through an optimal surface detection based on graph theory. Although the three SSM-based methods aforementioned perform well on liver segmentation, they require a complicated and time-consuming model construction process.

Recently, the auto context model (ACM) has been proposed in [32] to automatically segment subcortical structures from brain images. It integrates image appearances together with the context information (implicit shape model) by learning a series of classifiers. The classifier may choose two types of features: 1) image appearance features computed on the local image patches; and 2) context features from a large number of sites on the classification maps. Given a set of training images and their corresponding label maps, the first classifier is learned based on image appearance features. The classification maps created by the current classifier are then used as context information, along with image appearance features, to train the next classifier. The algorithm iterates to make the classification maps approximate the ground truth. In testing, the algorithm follows the same procedure by applying the sequence of learned classifiers to compute the classification maps. In [32], ACM has been proven powerful for brain image segmentation (both single structure segmentation and whole brain segmentation).

More recently, an ACM and multi atlases-based segmentation framework has been proposed for prostate

segmentation from CT images [33] and hippocampus segmentation from MR images [34], and got very impressive results. Motivated by the authors of [32]–[34], in this paper, I present an ACM-based algorithm for automatic liver segmentation from 3-D CT images, by using ACM, multi atlases, and mean-shift techniques. I try to apply the ACM and multi atlases-based segmentation framework described in [33] and [34] to liver segmentation from CT images and moreover an improved mean-shift over segmentation is used to speed up segmentation. Specifically, in the training stage, ACM is performed to construct a sequence of classifiers in each atlas space (based on each atlas and other aligned atlases). With the use of multiple atlases, I can obtain multiple sequences of ACM-based classifiers. In the segmentation stage, the test image will be first aligned onto each atlas space, and then segmented by the corresponding sequence of ACM-based classifiers. The final segmentation result will be obtained by fusing multiple segmentation results from multiple atlases via a fuzzy integral-based multi classifier fusion. Furthermore, in order to speed up segmentation, given a test image, I first use an improved mean-shift algorithm to perform over segmentation and then implement the region-based image labeling instead of the original inefficient pixel-based image labeling. The proposed method is evaluated on the datasets of MICCAI 2007 liver segmentation challenge. The experimental results show that our method is comparable to the state-of-the-art works on liver segmentation in terms of both accuracy and efficiency.

The main contribution of this paper is threefold: First, I introduce the ACM and multi atlases-based segmentation framework into liver segmentation from 3-D CT images. Second, I use the fuzzy integral to fuse the segmentation results from multiple atlas spaces. Third, an improved mean-shift over segmentation is employed to speed up liver segmentation.

The remainder of this paper is structured as follows: Section II describes the proposed ACM-based liver segmentation algorithm in detail. Section III evaluates the proposed method on the datasets of MICCAI 2007 liver segmentation challenge. Section IV concludes the paper.

II. METHOD

In this section, I present in detail the proposed ACM-based liver segmentation algorithm. The ACM integrates image appearance together with the context information (implicit shape model) by learning a series of classifiers, which avoids complicated procedures to construct an explicit SSM, and it has been successfully applied to brain and prostate segmentation. Thus, in this paper, I try to employ ACM as the primary tool for automatic liver segmentation from 3-D CT images.

A. Learn the Classifiers in Each Atlas Space by ACM

In the learning stage, a set of abdominal 3-D CT training images $\{X_j\}$ and the corresponding manual liver labels $\{Y_j\}$ are employed as the training set, where $j = 1, \dots, m$. Each training image is treated as an atlas and our task is to construct a sequence of classifiers by ACM in each atlas space.

To construct the sequence of classifiers in the space of one atlas X_a , the other $(m - 1)$ atlases X_b s need to be aligned with X_a by affine registration and the corresponding manual liver labels are also aligned. Thus, the set of abdominal CT training images $\{aX_j\}$ and the corresponding manual liver labels $\{aY_j\}$ in the space of X_a are obtained. Based on $\{aX_j\}$ and $\{aY_j\}$, I am able to construct the sequence of classifiers in the space of X_a by ACM.

1) Training of ACM: Similarly to [32], ACM first constructs a training set

$$S = \{(ayji, aXj(Ni)), j = 1, \dots, m, i = 1, \dots, n\} \quad (1)$$

where m is the number of training images, n is the number of pixels in each image, $ayji$ is the class label for pixel i in image aX_j , and $aX_j(Ni)$ denotes the local image patch centered at pixel i in image aX_j . The first classifier is learned based on the image appearance features computed on the local image patches $aX_j(Ni)$. For each training image aX_j , the classification maps P_j are then computed by the learned classifier. The algorithm then constructs a new training set

$$S^t = \{(ayji, (aX_j(Ni), P_j(i))), j = 1, \dots, m, i = 1, \dots, n\} \quad (2)$$

Where $P_j(i)$ is the classification map centered at pixel i for image aX_j . A new classifier is then trained, not only based on the image features extracted from $aX_j(Ni)$, but also on the context features extracted from $P_j(i)$. Once a new classifier is obtained, the algorithm repeats the same procedure until convergence. Figure. 1 gives an illustration of the training procedure of ACM. Finally, ACM outputs a sequence of learned classifiers

$$p(t)(yi / X(Ni), P(t-1)(i)), t = 1, \dots, T \quad (3)$$

where $P(0)$ is a uniform distribution, and thus the context features are not selected by the first classifier, i.e.,

$$p(1)(yi / X(Ni), P(0)(i)) = p(1)(yi / X(Ni)).$$

Due to the natural feature selection and fusion capability of the boosting algorithms, in this paper, I employ Ada Boost [35] as the basic classifier and I set the iteration number $T = 4$. The

Ada Boost classifiers automatically select and fuse important supporting context features, together with image appearance features. The same training procedure of ACM will be performed in each atlas space. Thus, I will obtain m sequences of learned classifiers, which correspond to the total m atlases.

2) Image Appearance and Context Features:

As aforementioned, I need to extract two types of features: 1) image appearance features; and 2) context features. In this paper, the image appearance features I employed include intensity, intensity mean, spatial positions

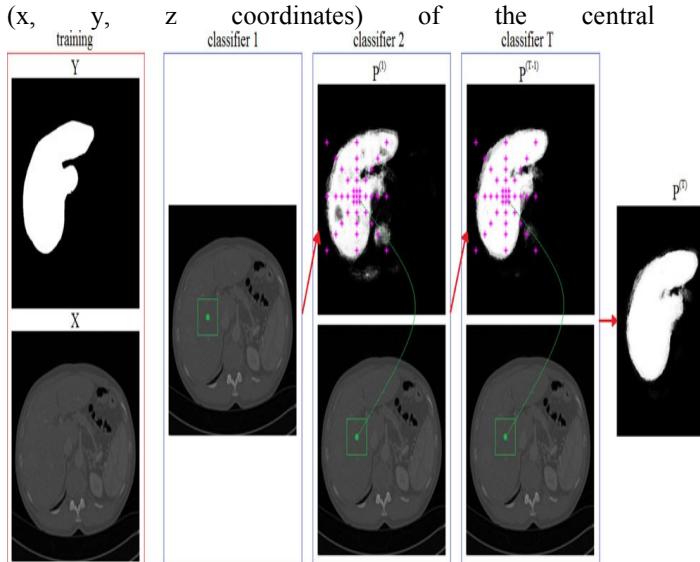


Figure. 1. Illustration of the training procedure of ACM. Given a set of abdominal CT training images and the corresponding manual liver labels, the first classifier is learned based purely on the local image appearance. The subsequent classifiers are learned not only based on the local image appearance, but also on the context features extracted from the classification map produced by the previous classifier. Objects with strong appearance cues are often correctly classified even after the first round. These probabilities then start to influence their neighbors in the next round (via context features), especially if there are strong correlations between them. Note that this is just a 2-D illustration. In fact, I use 3-D image and context features as detailed in Section II-A2

pixel of the local image patch, and various 3-D Haar features extracted from the local image patch. The image patch size I used is $7 \times 7 \times 7$. The 3-D context features are obtained from the 3-D classification maps, which is similar to the 2-D context feature extraction in [32]. For the 2-D applications in [32], eight rays in 45° intervals I stretched out from the current pixel of interest and the 2-D context locations I re sampled on these rays. In the case of our 3-D liver segmentation application, I extend the 2-D operation into the 3-D case, i.e., for each pixel of interest, 26 rays in directions of 26 neighbors are stretched out from the current pixel and a radius sequence (0, 1, 3, 5, 7, 10, 12, 15, 20, 25, 30, 35, 40, 45, 50, 60, 70, 80, 90, 100, 125, 150, 175, 200) is then used for sparsely sampling the 3-D context locations on each ray. The classification probabilities on these locations are used as context features (both individual probabilities and the mean probabilities within a $3 \times 3 \times 3$ window). Figure. 2 gives an illustration. The context features play a very important role in 3-D liver segmentation, due to the relatively fixed positions of abdominal anatomical structures.

B. Multiatlases-Based Liver Segmentation

1) Liver Segmentation in Each Atlas Space: In the segmentation stage, given a test image X_{test} , our task is to segment X_{test} in each atlas space. Let us take the space of atlas X_a , for example. First the test image X_{test} will be

aligned onto the space of X_a to obtain the aligned test image X_{test} . Then, a X_{test} will be segmented (each pixel in a X_{test} will be labeled) by the corresponding sequence of ACM-based classifiers in the space of X_a to obtain a classification map Y_{test} . Note that the segmenting procedure of ACM follows the training procedure of ACM by applying the sequence of learned classifiers to compute the classification maps, as shown in Figures. 3 and 4.

2) Results Fusion by Fuzzy Integral: The same segmenting procedure will be conducted in each atlas space as described in Section II-B1. Thus, I will obtain m final classification maps, corresponding to the total of m atlases. Finally, the m classification maps will be first transformed onto the original test image space, and then fused together by a multiclassifier fusion technique.

In this paper, I adopt the Choquet fuzzy integral [36] to fuse the classification maps from multiple sequences of classifiers. Fuzzy integral is a nonlinear fusion method in a decision making environment. It considers both the evidence supplied by each classifier and the importance of each subset of classifiers (via a fuzzy measure). Due to the non additivity of the adopted fuzzy measure, it can also represent the interaction among different classifiers. Fuzzy integral, as an aggregation tool in multi classifier fusion, has been widely used for pattern recognition, object classification, and object history matching [37], [38].

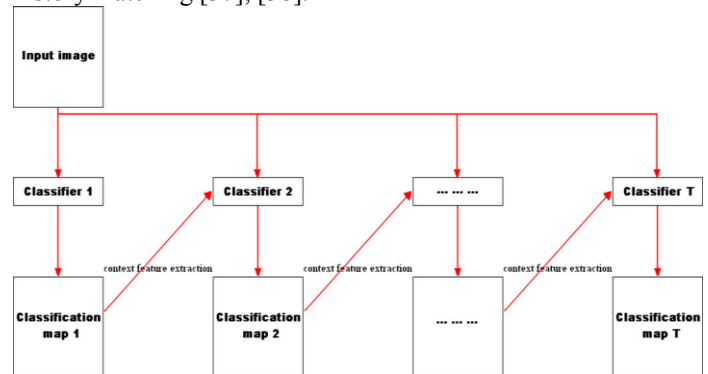


Figure. 2. Illustration of the segmenting procedure of ACM.

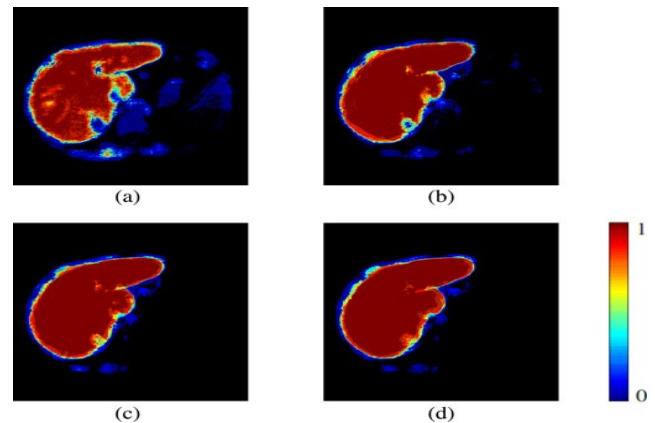


Figure. 3. Classification map of liver at each iteration of ACM. (a) Iteration 1. (b) Iteration 2. (c) Iteration 3. (d) Iteration 4.

C. Region-Based Labeling Using the Improved Mean-Shift Over Segmentation

Pixel-based image labeling is not efficient because it has to scan every pixel in the image. Especially, in our multi atlases based segmentation framework, it also has to scan the image many times.

In order to speed up segmentation, I use region-based image labeling instead of pixel-based image labeling. Specifically, given a test image, I first use the mean-shift algorithm [43] to perform over segmentation, to obtain a series of irregular image regions. For each region, a set of pixels (around 5%) are then randomly selected to perform classification. I take the average of the classification probabilities of these sampled pixels as the probability of the region (assigning all pixels in the region with such a probability).

Also, in the training stage, I can use only the sampled pixels in all regions to train the classifiers, which drastically reduce the training time.

However, due to the high intensity similarity between liver tissue and adjacent organs (such as heart and stomach) in abdominal CT images, sometimes even the standard mean-shift over segmentation cannot separate them. Figure 5 gives an illustration of the standard mean-shift over segmentation. As I can see from Figure 5, the intensities of the liver and the adjacent heart are highly similar, which makes it difficult to separate the liver from the heart by the standard mean-shift algorithm.

In order to tackle such a problem, I introduce prior probability as an additional feature for the mean-shift algorithm. In this way, leakage of image regions pertaining to the liver into

surrounding tissue can be avoided. The prior probability map is obtained by taking the average of aligned manual liver labels of all the training images. In other words, during the over segmentation stage, I attempt to separate liver tissue from adjacent organs (such as heart and stomach) based on empirical knowledge derived from all known manual liver labels. Specifically, I apply the 5-D mean-shift over segmentation using three dimensions for the x, y, z coordinates, one dimension for intensity and one dimension for prior probability. The kernel I used is the uniform one. Figure 6 gives an illustration of the improved mean shift over segmentation. As I can see from Figure 6, although the improved mean-shift algorithm further over segments the image, it can separate the liver tissue from the heart (based on empirical knowledge).

D. Outline of the Algorithm

Here, I give the outline of our final algorithm. In training, given a set of abdominal CT training images (atlases) along with the corresponding manual liver labels, ACM is performed to learn a sequence of classifiers in each atlas space (based on each atlas and other aligned atlases). Thus, after training, multiple sequences of ACM-based classifiers are obtained. In testing, given a test image: 1) Align the test image onto each atlas space. 2) In each atlas space, over segment the aligned test image using the improved mean-shift algorithm to obtain a series of irregular image regions. 3) Perform region-based classification using

the corresponding sequence of ACM-based classifiers. 4) Obtain the final segmentation result by fusing all classification results from all atlas spaces by the fuzzy integral. Note that, practically, I perform mean-shift over segmentation only in one atlas space. The over segmentation results in other atlas spaces can be achieved by applying an affine transformation between the atlases.

III. EXPERIMENTS

A. Experimental Data and Setup

I evaluate our learning-based liver segmentation method on the training and testing datasets of MICCAI 2007 liver segmentation challenge (<http://www.sliver07.org>). There are 20 contrast-enhanced abdominal CT images in the training datasets, and 10 in the testing datasets. All images have a spatial resolution of 512×512 pixels in each transversal slice and the pixel spacing varies from 0.55 to 0.9 mm. The inter slice distance varies from 0.5 to 5 mm.

Figure 5. Illustration of the standard mean-shift over-segmentation. (a) One original transversal slice. (b) Over segmentation result using the standard mean-shift algorithm.

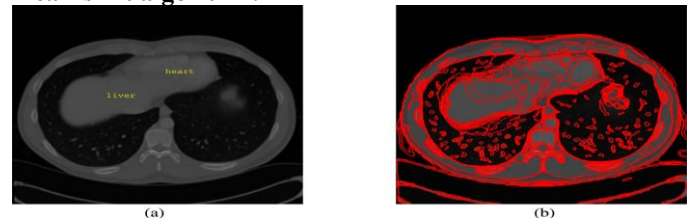
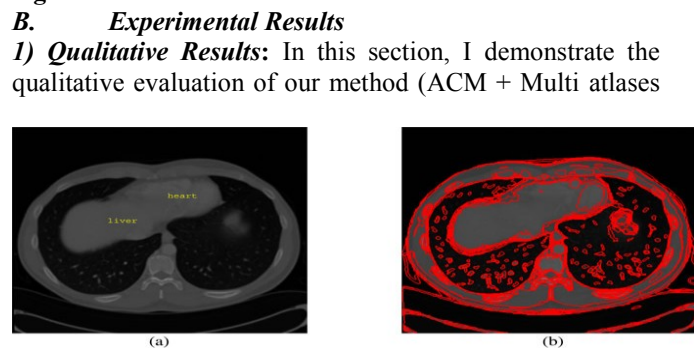


Figure 6. Illustration of the improved mean-shift over segmentation. (a) One original transversal slice. (b) Over segmentation result using the improved mean-shift algorithm.



+mean-shift). I compare our method with the methods using Only ACM and using ACM in the multi atlases based framework. Note that, for the method using only ACM, I randomly select one atlas space and learn the classifiers by ACM in that space. For fair comparison, the same parameters are employed in ACM for all the methods. The comparison results are shown in Figure 7. From Figure 7, I can observe that the segmentation results by the method using ACM in the multi atlases-based framework are closer to the manual reference segmentations than those by the method using only ACM, and the segmentation results by our method are comparable to those by the method using ACM in the multi atlases-based framework. However, our method is significantly faster as detailed in the next section.

2) Quantitative Results: For quantitative evaluation of our method, the following five evaluation metrics from the MICCAI 2007 workshop [30] are adopted: volumetric overlap error, signed relative volume difference, average symmetric surface distance (DAvg), root mean square symmetric surface distance (DRMS), and maximum symmetric surface distance (DMax). I also include runtime as an additional measure for efficiency evaluation.

IV. CONCLUSION

In this paper, I have presented an ACM-based algorithm for segmenting liver from 3-D CT images. Specifically, by combining ACMs and a multi-atlases technique, multiple sequences

of ACM-based classifiers are constructed, and further used for liver labeling. The final segmentation result will be obtained by fusing multiple segmentation results from multiple sequences of classifiers via a fuzzy integral based multi-classifier fusion. In order to speed up segmentation, I also introduce an improved mean-shift algorithm to over-segment the test image and subsequently perform a region-based image labeling instead of the original inefficient pixel-based image labeling. The proposed method has been evaluated on the datasets of MICCAI 2007

liver segmentation challenge. The experimental results show that our method is comparable to the state-of-the-art work on liver segmentation in terms of both accuracy and efficiency.

REFERENCES

- [1] H. Lamecker, T. Lange, and M. Seebae, "Segmentation of the liver using a 3D statistical shape model," Zuse Inst., Berlin, Germany, Tech. Rep. 04-09, pp. 1-25, 2004.
- [2] D. Kainmuller, T. Lange, and H. Lamecker, "Shape constrained automatic segmentation of the liver based on a heuristic intensity model," in Proc. Mid. Image Comput. Comput.-Assisted Intervention Workshop 3-D Segmentation Clinic Grand Challenge, 2007, pp. 109-116.
- [3] T. Heimann, H.-P. Meinzer, and I. Wolf, "A statistical deformable model for the segmentation of liver CT volumes," in Proc. Mid. Image Comput. Comput.-Assisted Intervention Workshop 3-D Segmentation Clinic Grand Challenge, 2007, pp. 161-166.
- [4] X. Zhang, J. Tian, K. Deng, Y. Wu, and X. Li, "Automatic liver segmentation using a statistical shape model with optimal surface detection," IEEE Trans. Biomed. Eng., vol. 57, no. 10, pp. 2622-2626, Oct. 2010.
- [5] H. Badakhshannoory and P. Saeedi, "A model-based validation scheme for organ segmentation in CT scan volumes," IEEE Trans. Biomed. Eng., vol. 58, no. 9, pp. 2681-2693, Sep. 2011.
- [6] H. Park, P. Bland, and C. Meyer, "Construction of an abdominal probabilistic atlas and its application in segmentation," IEEE Trans. Med. Imag., vol. 22, no. 4, pp. 483-492, Apr. 2003.
- [7] X. Zhou, T. Kitagawa, K. Okuo, T. Hara, H. Fujita, R. Yokoyama, M. Kanematsu, and H. Hoshi, "Construction of a probabilistic atlas for automated liver segmentation in non-contrast torso CT images," Int. J. Comput. Assist. Radiol. Surg., vol. 1281, pp. 1169-1174, 2005.

[8] D. Furukawa, A. Shimizu, and H. Kobatake, "Automatic liver segmentation based on maximum a posterior probability estimation and levelset method," in Proc. Mid. Image Comput. Comput.-Assisted Intervention Workshop 3-D Segmentation Clinic Grand Challenge, 2007, pp. 117-124.

[9] L. Gao, D. Heath, and E. Fishman, "Abdominal image segmentation using three-dimensional deformable models," Investigative Radiol., vol. 33, no. 6, pp. 348-55, 1998.

[10] L. Soler, H. Delingette, G. Malandain, J. Montagnat, N. Ayache, C. Koehl, O. Dourthe, B. Malassagne, M. Smith, D. Mutter, and J. Marescaux, "Fully automatic anatomical, pathological, and functional segmentation from CT scans for hepatic surgery," Comput. Aided Surg., vol. 6, no. 3, pp. 131-142, 2001.